Proceedings of ASME Power 2006
May 2-4, 2006, Atlanta, Georgia, USA

PWR2006-88079

EFFECTS OF HYDROGEN ENRICHMENT ON CONFINED METHANE FLAME BEHAVIOR

Onur Tuncer[†]
Department of Mechanical Engineering,
Louisiana State University, Baton Rouge, LA, 70803
otunce1@lsu.edu

Sumanta Acharya[‡]
Department of Mechanical Engineering,
Louisiana State University, Baton Rouge, LA, 70803
acharya@me.lsu.edu

Jong Ho Uhm[#]
Department of Mechanical Engineering
Louisiana State University, Baton Rouge, LA 70803
jhuhm@lsu.edu

ABSTRACT

Many land based power generation units presently operate on natural gas, whose major constituent is methane, and many of them would need to tackle the challenges due to a fuel switch towards synthesis gas in the near future. Operating conditions and stability of a pre-mixed gas turbine combustor is quite sensitive to the changes in the fuel composition. Behavior of a premixed confined hydrogen enriched methane flame is studied with regard to thermo-acoustic instability induced flame flashback, emissions, flammability limits and acoustics over a wide range of operating conditions. However, most emphasis is put on lean combustion, which is an industry standard method used to lower pollutant emissions by reducing adiabatic flame temperatures. Hydrogen addition extends the flammability limits and enables lower nitric oxide emissions levels to be achieved at leaner equivalence ratios. On the other hand, increased root-mean-square pressure fluctuation levels, and higher susceptibility to flashback is observed with increasing hydrogen volume fraction inside the fuel mixture. This phenomenon is mostly attributed to much higher burning speeds of hydrogen in contrast to pure methane. A semi-analytical model has been utilized to capture the flame holding and thermo-acoustically induced flame flashback dynamics for a pre-mixed gas turbine combustor. A simple linearized acoustic model, derived from the basic conservation laws, and a front-tracking algorithm based on the Markstein's G-equation are coupled together in order to track the flame initiation front, which in turn yields in an understanding of dynamic flame holding characteristics. A limit cycle behavior in the flame front movement is observed during simulations due to a non-linearity in the feedback term that relates acoustic velocity to heat release. Sets of experiments including flashback speed measurements have been performed at varying fuel composition. Phase locked CH radical imaging measurements have also been performed in order to track the flame initiation front in time with respect to the dominant instability cycle. Computer simulations are performed to study flashback and combustor acoustics together numerically and it is observed that these are in good qualitative agreement with the experiments.

NOMENCLATURE

A	Cross sectional area / Flame area
a	Fuel exponent
B	Pre-exponential factor
b	Oxidizer exponent
c	Speed of sound
c_p	Specific heat at constant pressure
D	Combustor diameter
e	Internal energy per unit mass
E_a	Activation energy
f	Flame front function
h	Enthalpy
k	Wave number
K_f	Overall forward reaction rate
L	Flame height / Combustor length
n	Temperature exponent
P	Pressure
q	Heat release

[†] Graduate Student, Corresponding Author
[‡] L.R Daniel Professor
[#] Research Associate

R	Gas constant
S	Flame speed
T	Temperature
t	Time
u	Longitudinal velocity
x	Longitudinal coordinate
z	Axial flame coordinate
Δt	Time step
Δx	Grid spacing

Greek Symbols

ϕ	Equivalence ratio
ω	Frequency
α	Thermal diffusivity
β	Zel'dovich parameter
γ	Specific heat ratio
δ	Delta function
ρ	Density
ψ	Mode shape

Subscripts

ad	Adiabatic
air	Air
d	Downstream with respect to flame position
f	Flame
fuel	Fuel
in	Inlet
L	Laminar
T	Turbulent
u	Upstream with respect to flame position

Superscripts

$\bar{}$	Time average
$(.)'$	Fluctuating quantity
.	Time derivative

INTRODUCTION

Gas turbine engines are commonly utilized in electricity generation [1]. These modern premixed gas turbine combustors are usually operated very close to the lean blowout limit due to emissions considerations [1]. Lean combustion reduces the adiabatic flame temperature thus reducing the production rate of nitric oxides which is a highly temperature dependent process [2]. As the adiabatic flame temperature is lower carbon monoxide emissions tend to increase. Therefore an optimum operating point needs to be sought to guarantee both low nitric oxide and carbon monoxide emissions. In this operating range flame holding and thermo-acoustic instability become the two most important considerations. Thermo-acoustic instability not only deteriorates the material structure of the combustor wall subjecting it to fatigue loading [3], but also can induce hazardous flame flashback into the premixing section [4]. From this point of view near lean blowout behavior of syngas needs to be explored in a detailed manner.

Thermo-acoustic oscillations occur because unsteady heating generates sound waves that produce velocity and pressure perturbations. Inside a combustor these oscillations again couple with the heat release [3]. If the unsteady heat input is in phase with pressure perturbations acoustic waves gain energy and instability becomes possible. In his pioneering work Lord Rayleigh [5] presents a clear physical description of this self-excitation phenomenon. In reality, strength of these oscillations are limited by non-linear effects such as flame hydrodynamics and limit cycle oscillations occur. However, these oscillations can be so strong that they can even cause gas turbine to shut down in order to avoid catastrophic damage. These pressure fluctuations can reduce the lifetime of gas turbine hardware. Thermo-acoustic fluctuations also have an effect on flame stability and flame holding. During these oscillations flame boundary also moves [6] as well. Note that even the location of the flame-front has an effect on stability characteristics [7]. If adequate conditions are present flame might enter inside the premixing section triggering flashback. This phenomenon is called as thermo-acoustic instability induced flame flashback. For the study of thermo-acoustic instability often the flame is assumed to anchor at a specific point inside the combustor. This assumption is likely to be satisfied in well-stabilized flames [8], however this paper deals with resolving ill behavior due to poor flame stability. Enabling the flame front to move is the only way to study such behavior. On the other hand this approach lacks the fidelity of resolving flame front movement and capturing erratic behavior such as flashback or poor flame holding due to self-excited oscillations.

Synthesis gas, a clean source of energy, is a variable mixture of primarily hydrogen (H_2) and carbon monoxide (CO). Energy contribution of syngas in the existing integrated cycle (IGCC) land power generation installations is roughly10-20% of the total power output. Depending on the gasification process variables and which solid is gasified (biomass or coal) substantial change in the resulting syngas composition can occur [9]. This change in the syngas composition significantly alters the flame behavior [10]. The quality and composition of the fuel impacts the turbine life and emissions [11]. Therefore characterization flame behavior at different syngas compositions is an extremely important task. In addition, syngas combustion in particular generates many of the adequate conditions for flashback due to high flame speeds associated with its hydrogen content. For example under normal conditions laminar flame speed of a stoichiometric methane air mixture is about 40 cm/s whereas this speed is about 200 cm/s for a stoichiometric hydrogen air mixture. Therefore hydrogen flame propagates roughly five times faster than a methane flame. This mismatch between flame speeds manifests itself as flame holding problems in a gas turbine engine environment.

In order to achieve a desired power output from syngas high mass flow rates need to be used, since it is a low BTU fuel. High mass flow rates normally translate into higher injection speeds, which pose a significant problem in terms of flame holding [12, 10, 13, 14].

The aim of this paper is to develop a simplified mathematical model for flame holding and thermo-acoustic instability induced type flame flashback and to verify it against experimental data. Obviously this type of flashback is not the only one that occurs in combustors. Other flashback types include boundary layer propagation, flashback due to low flow speeds and combustion induced vortex breakdown (CVIB) type flashback.

MATHEMATICAL MODEL

Under the main underlying assumptions of inviscid, one-dimensional flow, ideal gas, and finally negligible pressure losses along the length of the combustor, equation that governs the dynamics of acoustic wave motion inside the combustor tube can be given as follows (see Eq.1). Near the flame acoustic field in a real combustor is in fact two-dimensional but this two-dimensionality of the field has no impact on flame behavior [8].

$$\frac{\partial^2 P}{\partial t^2} + c^2 \frac{\partial^2 P}{\partial x^2} = (\gamma - 1)\frac{\partial q'}{\partial t} \quad (1)$$

While solving this wave equation, fully non-reflecting and fully reflecting boundary conditions are used for closed inlet and open outlet respectively. The boundary condition imposed by the closed end of the tube is that air particles at the closed end cannot move back and forth since they are adjacent to a wall. Contrarily at the open end of an acoustic tube, a standing wave has maximum fluctuation in volume velocity, but zero variation in air pressure. These boundary conditions (Eq. 2-3) represent the situation inside the combustor tube realistically.

$$u'(0,t) = 0 \quad (2)$$

$$P'(L,t) = 0 \quad (3)$$

In general for a fully premixed flame, combustion occurs within a thin interface that separates fresh and burnt gases. For a one-dimensional situation as in here flame front can be modeled as an infinitely thin plane. This assumption is satisfied on the condition that the axial extent of heat release is much smaller in comparison with the acoustic wavelength [3]. In practice combustor is usually a small part of a much large inlet outlet ducting system such that this assumption is justified. Therefore heat release is concentrated at the downstream end of the flame.

$$\rho(x) = \begin{cases} \rho_u & x \le x_f \\ \rho_d & x > x_f \end{cases}$$

$$c(x) = \begin{cases} c_u & x \le x_f \\ c_d & x > x_f \end{cases} \quad (4)$$

$$T(x) = \begin{cases} T_{in} & x \le x_f \\ T_{ad} & x > x_f \end{cases}$$

Density, speed of sound and temperature are constant in either side of the flame (Eq 4). Flame front represents a discontinuity over which a sudden jump occurs in these properties. Considering the nature of premixed flames this assumption is a valid one and is often used to simplify the analysis.

Expressing pressure as the product of a time dependent amplitude and spatial mode shape function, which satisfies the boundary conditions the partial differential equation, can be simplified into an ordinary differential equation. In reality, there exist more than one admissible mode shape yet one can assume a single dominant mode is present.

$$P'(x,t) = \bar{P}\,\eta(t)\psi(x) \quad (5)$$

Furthermore the acoustic velocity u' can be expressed as follows,

$$u'(x,t) = \dot{\eta}(t)\frac{\partial \psi(x)}{\partial x}k^{-2} \quad (6)$$

Now Eq. 1 can be transformed into the following form.

$$\ddot{\eta} + \omega^2 \eta = \frac{(\gamma - 1)}{\bar{P}} E^{-1} \frac{dq'}{dt} \quad (7)$$

where E is defined as,

$$E = \int_0^L \psi^2(x)dx \quad (8)$$

Mode shape of pressure is given by,

$$\psi(x) = \begin{cases} \cos\left(\frac{\omega x}{c_u}\right) & x \le x_f \\ \frac{\cos(\alpha)}{\sin(\beta)}\sin\left(\frac{\omega(L-x)}{c_d}\right) & x > x_f \end{cases} \quad (9)$$

where,

$$\alpha = \omega\, x_f / c_u \quad (10)$$

$$\beta = \omega\,(L - x_f)/c_d \quad (11)$$

Lowest possible frequency of oscillation is the smallest root of the below equation.

$$\tan\alpha \tan\beta = (\rho_u c_u)/(\rho_d c_d) \quad (12)$$

On the right hand side of Eq. 1 unsteady heat release rate appears. This is the term that determines the nature of coupling between heat release and pressure perturbations. For a premixed flame as in this case reaction time is much faster than period of acoustic fluctuations so that heat input responds quasi-steadily to the changes of flow rate (thus velocity) coming into the flame front.

A level set based front tracking method is used to resolve flame front dynamics. Premixed flame stabilizes on the fuel injector tip, which acts like a center-body. Assuming an axisymmetric flow field and further assuming that combustion occurs on a surface whose axial position is given by a single-valued function $z = f(r,t)$, flame surface can be defined by a level-set of the well-known G-equation $G(z,r,t) = 0$. G-equation allows one to decouple dynamics of the reacting flow field from chemistry [15].

$$G(z,r,t) = z - f(r,t) \quad (13)$$

Neglecting the radial component of velocity as both the mean and fluctuating (acoustic) component of the velocity were assumed to be one dimensional level set equation that governs the flame front movement can be written in the following form as,

$$-\frac{\partial f}{\partial t} + u = S_L\left(1 + \left(\frac{\partial f}{\partial r}\right)^2\right)^{1/2} \quad (14)$$

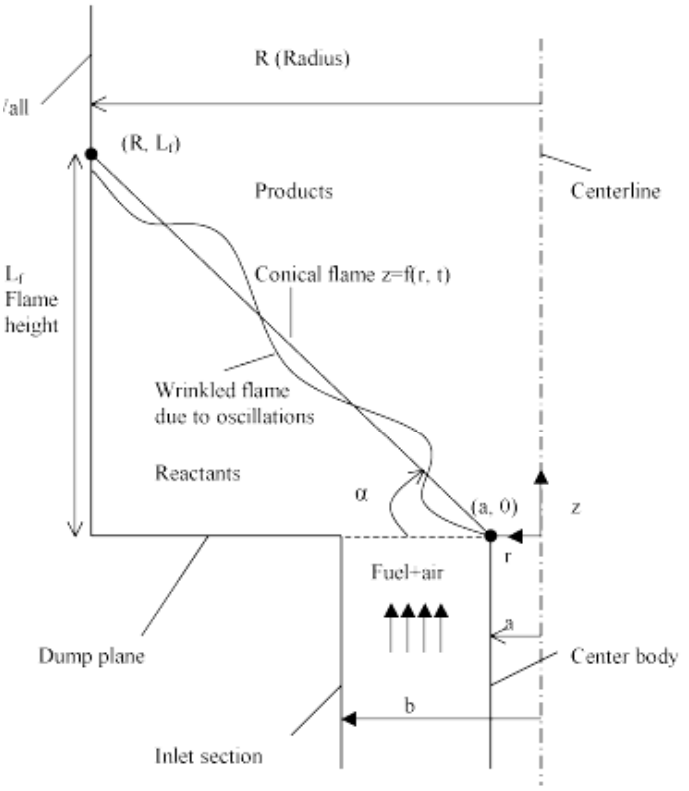

Figure 1 Geometry of the Flame

Self-excited oscillations in a ducted can be sufficiently intense, so that reverse flow can occur [16]. For flow velocities less than flame speed flame cannot remain attached at the tip and starts to propagate downstream. Therefore the boundary condition of Eq. 15 at $r = a$ should take this flashback phenomenon into consideration. In addition to de-attachment flame remains perpendicular to the center body to assure zero normal velocity on the wall of the flame-holder on both sides of the flame. Eq. 15 as per [16] prescribes the appropriate boundary conditions for the flame-front equation. Apparently there is a certain hysterisis associated with this boundary condition treatment. Such hysterisis effect however is observed in the Schlieren images of Jones [17].

$$\left.\frac{\partial f}{\partial r}\right|_{r=a} = \begin{cases} \dfrac{\left(u^2 - S_L^{\,2}\right)^{1/2}}{S_L} & if \quad u(t) \geq S_L \wedge \quad f(a,t) = 0 \\ 0 \quad if \quad u \leq S_L \vee \quad f(a,t) < 0 \end{cases} \qquad 15$$

Laminar flame speed appearing in the above equations can be easily obtained from basic theory. Laminar flame speed S_L is a function of Zel'dovich parameter, thermal diffusivity and the forward reaction rate K_f.

$$S_L = \sqrt{2\beta^{-2}\alpha K_f} \qquad 16$$

where the Zel'dovich parameter β is expressed as,

$$\beta = \frac{E_a}{R_u T_{ad}^{\,2}}\left(T_{ad} - T_{in}\right) \qquad 17$$

and the forward reaction rate is given by a one-step global chemistry approximation in Eq. 18.

$$K_f = B.[Fuel]^a[Oxidizer]^b T^n \exp\left(-E_a/RT\right) \qquad 18$$

For a mixture of gases flame is assumed to propagate at a speed associated with the component that has the highest flame speed. For synthesis gas this component is hydrogen most of the time above a certain hydrogen concentration within the fuel blend. Table 1 shows the reaction rate parameters such as temperature exponent n, pre-exponential factor B and activation energy E_a. These parameters are used for the calculation of K_f that appears in the laminar flame speed equation (see Eq. 16).

Reaction	n	a	b	B	E_a
$CH_4 + 2O_2 = CO_2 + 2H_2O$	0	-0.3	1.3	$1.9.10^5$	48.4

Table 1 Reaction Rate Parameters

The very physical argument behind this is that the amount of unsteady heat release should be bounded by the amount of fuel available to be burnt. After all the fuel available at the flame location is consumed the unsteady heat release must in fact vanish.

The non-linearity in the feedback equation (Eq. 19) takes care of the desired non-linearity by gradually saturating the heat release in frequency domain. β is the static gain α is the cut-off frequency of the filter. These filter coefficients are obtained by Park et. al. by linearizing the heat release equation [18]. These parameters are functions of the operating conditions (equivalence ratio, residence time etc.). For small values of fluctuating mass flow rates the system behaves like a first order linear time invariant filter. However, at larger disturbances the term in parenthesis on the right hand side introduces a non-linearity by saturating the heat release output. Due to this saturation effect a stable limit cycle can be reached. This is consistent with the physical considerations outlined in the preceding paragraph.

$$\dot{q}'(s) = \frac{\beta}{s+\alpha}\dot{m}'(s)\left(1 - \left|\frac{\dot{m}'(s)}{\bar{\dot{m}}}\right|\right) \qquad 19$$

Original flame front level set equation is a type of Hamilton-Jacobi equation, which poses certain difficulties during numerical solution as it admits non-smooth solutions, which do not make any physical sense. For this reason flame front equation and the corresponding boundary condition are transformed into an equivalent weakly hyperbolic conservation equation form and discretized on a radial grid with a 5th order WENO scheme. Initial value of the flame front $f(z,0)$ is set to its time averaged conical position and integrated explicitly using a 3rd order Runge-Kutta method.

EXPERIMENTAL APPARATUS

In this section details of the experimental apparatus are discussed. Combustor shell that follows the inlet and premixing sections is comprised of two pieces. A 2.75" inner diameter quartz tube sits on a 316 stainless steel flange, which defines the dump plane. This quartz tube enables optical access to the main re-circulation zone. Design of this laboratory scale combustor represents actual premixed combustor designs. Combustor is operated up to a power rating of 20 kW. Quartz

tube and the stainless steel shell are cooled by means of forced convection during combustion.

Combustion air is fed through an eight-blade 45º-swirl vane (see Figure 2). A correlation [19] gives the corresponding swirl number as Sw= 0.98. Swirl provides stabilization at the dump plane and facilitates the entrainment of fuel jets within the cross flow at the pre-mixer. Swirling airflow is fully developed when it reaches the location of fuel injection. A typical axial air speed inside the premixer reaches 3 m/s for a 5 lt/s combustion airflow.

Hydrogen H_2 and methane CH_4 are individually supplied from compressed gas tanks and mixed inside a manifold before the combustor inlet (see Figure 2). Their flow rates are monitored by separate mass flow meters. Mass flow rates of carbon monoxide and hydrogen are adjusted separately to achieve the desired fuel composition. Air necessary for combustion is supplied from a 290psig, 450 ACFM air compressor. Volumetric airflow rate is measured by a rotameter and a pressure gage at the rotameter exit is used to correct the readings.

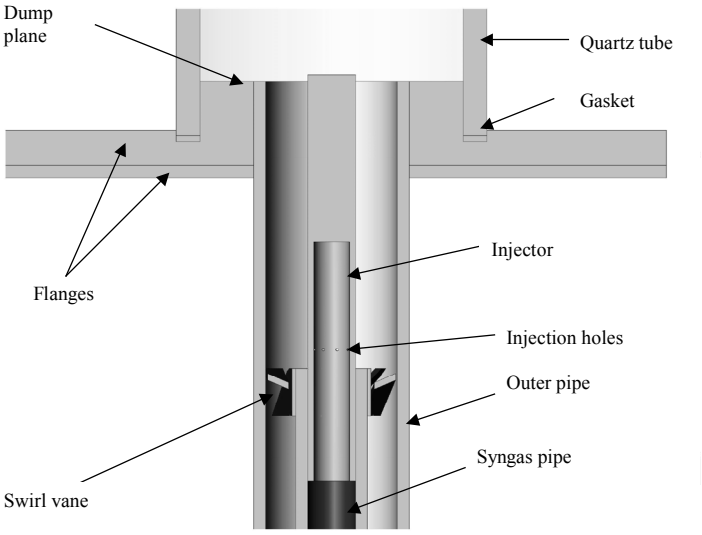

Figure 2 Schematic of the Syngas Delivery Section

RESULTS AND DISCUSSION

Preliminary measurements are taken using pure methane CH_4, major component of natural gas, in order to establish a baseline for syngas measurements. Natural gas has been in widespread use for a long time, and it needs to be substituted with other alternate fuels extending fuel flexibility and avoiding its sudden exhaustion. Syngas and hydrogen (SGH) fuels appear to be a substitutive remedy. On the other hand, as mentioned in the introduction section, combustion of SGH fuels has different technological needs since these fuels have much different combustion characteristics from natural gas such as flame behavior and emissions levels.

During measurements authors have slowly added hydrogen to methane with 10 % increments on a volume basis up to 50 % hydrogen content.

Combustor Operating Regimes

First, it is important to identify different operating regimes of the combustor prior to making detailed studies at desired load conditions. Figure 3 identifies distinct operating regimes as a function of equivalence ratio and total mass flow rates. Each symbol corresponds to a data point and boundaries are drawn on the figure in order to clearly identify the separate regimes. The pre-mixed combustor, exhibits near limit oscillations in the form of repetitive flame extinction and re-ignition within the close vicinity of lean and rich blowout equivalence ratio limits. Such behavior is very typical of gas turbine combustors especially for pre-mixed type ones. In between those two lies a distinct stable regime shown with diamond shaped symbols where the flame tip remains attached at the tip of the center body at all times. On the other hand flashback instability regime marked with rectangles is concentrated at two separate regions in either side of the stable region confined by one of the near limit behavior boundaries. In the event of flashback flame tip leaves the tip of the center body propagates upstream towards the pre-mixing region and re-attaches at the tip again. This behavior repeats itself. This type of ill behavior is encountered at relatively low or high mass flow rates. For low flow mass rates the axial flow velocity is lower which results in a narrower cone angle. Low ratio of u/S_L makes it easier for pressure fluctuations to detach the flame tip. Hence flashback can occur even at moderately low RMS pressure fluctuations. On the other hand flashback instability is also encountered at elevated mass flow rates, which in fact correspond to higher velocities and therefore steeper cone angles for the flame. At these operating conditions pressure pulsations are much stronger in the amplitude

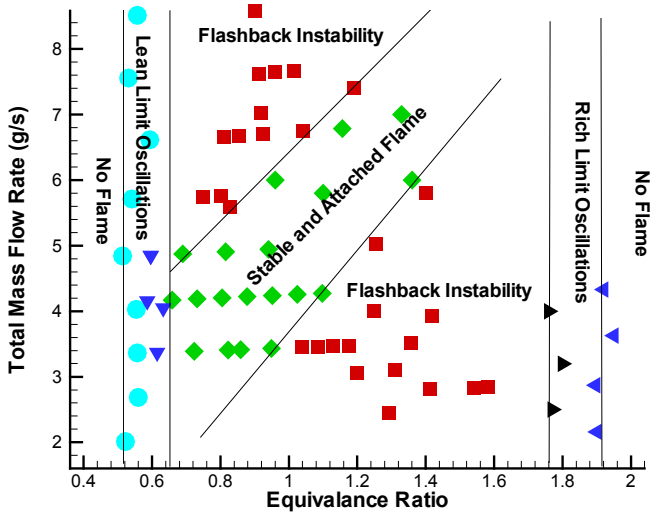

Figure 3 Combustor Operating Regimes (Pure CH_4)

In contrast to natural gas, synthesis gas flame has a much different flow behavior due to both different laminar flame speed and adiabatic flame temperature. Both laminar flame speed and adiabatic flame temperature heavily depend on syngas composition. Since there are multiple fuels in a methane and hydrogen mixture a suitable definition of the equivalence ratio, which takes the overall stoichiometry into account, is necessary. Following the assumptions of Yu et. al. [20] an equivalence ratio is defined as follows. This equation implies

that the hydrogen in the blend is completely oxidized and the remaining oxygen is used to burn the methane content, since the hydrogen oxidation proceeds much faster than methane oxidation.

$$\phi = \frac{C_F \Big/ \left[C_A - C_H \Big/ \left(C_H / C_A \right)_{st} \right]}{\left(C_F / C_A \right)_{st}} \qquad (20)$$

As mentioned in the introduction section today's gas turbine engines are operated near their lean blow-off limits due to emissions considerations. Here blow-off limits for the laboratory scale combustor are identified with respect to the particular choice of fuel or fuel composition for this reason. Hydrogen enrichment considerably extends the lean blowout limits of the methane fuel as evidence to this argument is shown in Figure 4. It is also seen that this blowout limit is not fixed but rather a function of mass flow rate, which is mostly related with the volumetric flow rate of combustion air. These effects regarding the extension of lean blowout limits through hydrogen addition are consistent with the recent observations reported by Schefer, Guo et. al. and Zhang et. al. [24, 25, 26].

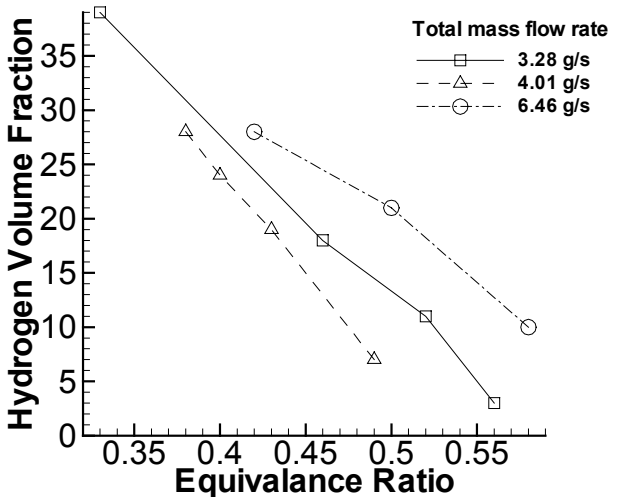

Figure 4 Effect of Hydrogen Enrichment on Lean Blowout Limit

Heat Release and Pressure Measurements

A number of water-cooled piezo-electric pressure transducers are mounted along the combustor wall measures dynamic pressure variations in the combustor. So as to examine the waveform of the combustion instability pressure inside the reactor is measured at several stations along the entire length of the combustor.

The CH radical light intensity is recorded using a photodiode looking at the flame equipped with an appropriate band-pass optical filter. Photodiode reading is taken as a measure of integral heat release fluctuations in the main reaction zone of the combustor.

Figure 5 shows the Fourier spectra of CH light and pressure signals. Both exhibit oscillatory behavior as governed by the acoustic modes of the combustor. These modes depend on the boundary conditions at the inlet and outlet. Interestingly a sudden shift in the dominant frequency occurs after certain hydrogen content within the fuel is exceeded. In Figure 6 one can identify two distinct regions one with high frequency and the other one with low frequency. To understand which modes

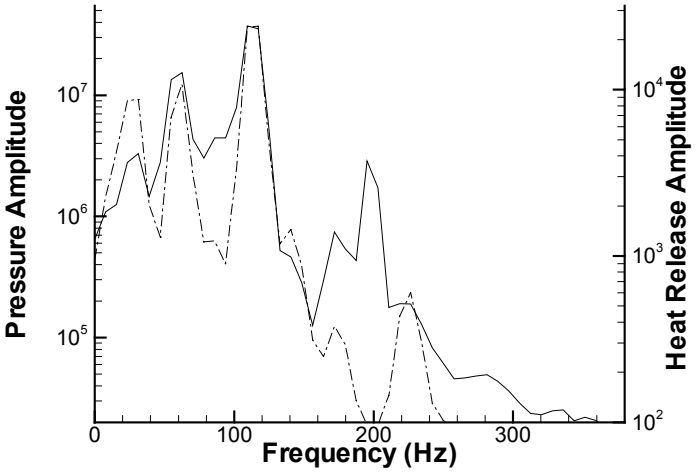

Figure 5 Heat Release and Pressure Spectra (ϕ=0.9, Q_{air}= 215 lpm, Solid Line, Pressure, Dashed Line, Heat Release)

each corresponds to one needs to have an idea about the acoustic mode shape. Therefore simultaneous pressure measurements are performed at these conditions with one of the sensors near the inlet and the other one being near the exit. Results (see Figure 7) indicate that the low frequency oscillations are associated with the bulk mode and the high frequency ones with the longitudinal mode. For the bulk mode the amplitude of the mode shape is constant whereas for the longitudinal mode it has maximum amplitude at the closed inlet

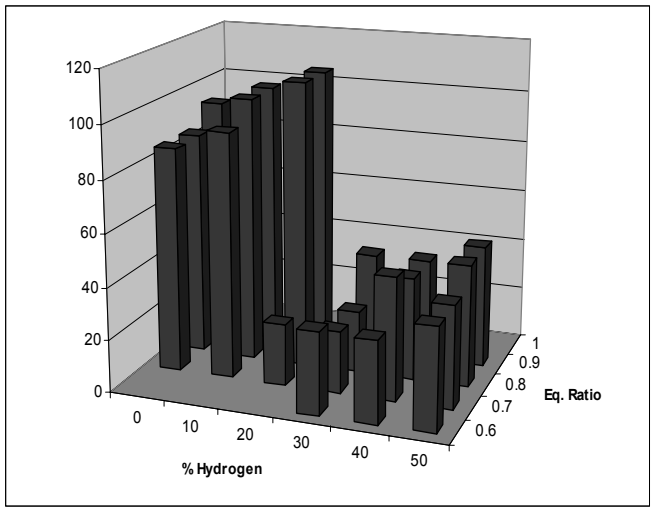

Figure 6 Dominant Frequency (Hz) with Respect to Fuel Composition and Equivalence Rate (Q_{air}=374 lpm)

and gradually decays to zero at the open outlet. So for the bulk mode pressure is same everywhere in the combustor and for the longitudinal mode the combustor acoustic pressure is lower

than the inlet acoustic pressure. The cause of this sudden change in the dominant mode is not understood and needs to be explored in detail as a topic of further research.

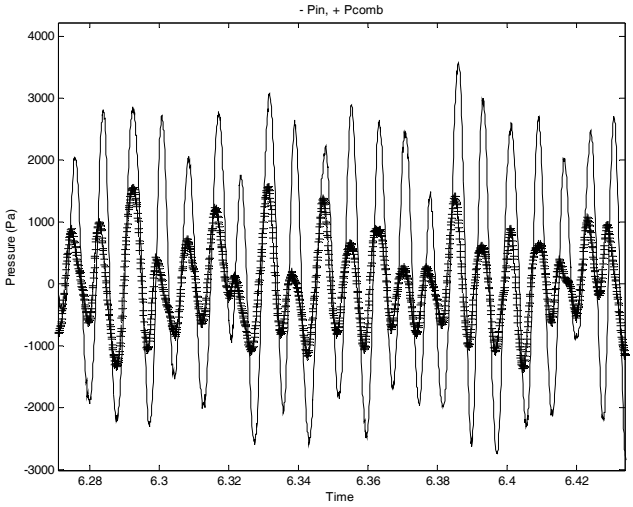

a. Longitudinal Mode

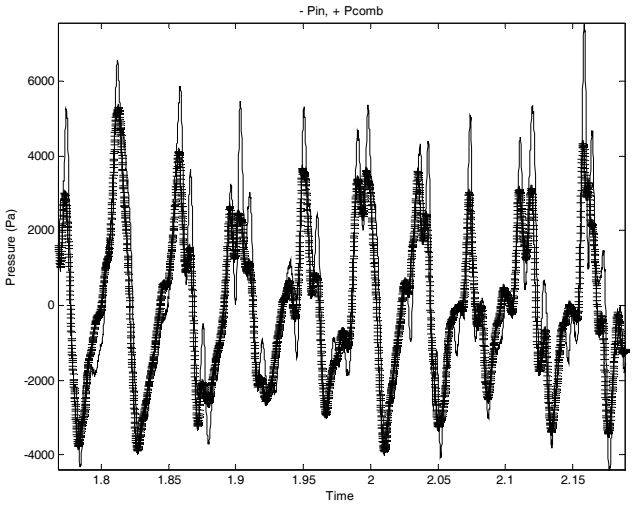

b. Bulk (Helmholtz) Mode

Figure 7 Spatial Dependence of Pressure Amplitude with Different Modes ("+", $P_{combustor}$,"-", P_{inlet})

RMS pressure amplitude is affected significantly by the fuel composition. Holding the other two parameters (equivalence ratio and total mass flow rate) constant enrichment of methane with hydrogen usually yields in higher amplitude pressure fluctuations (see Figure 8). This should be related to the more rigorous oxidation of the hydrogen content of the fuel blend. The dips at the RMS level observed at 50% H_2 for 184 and 253 lpm airflow rates correspond to a combustion regime change and therefore are irrelevant to this discussion. At these two points flame does not stabilize at the dump plane but rather stabilizes near the injector discharge holes within the pre-mixer. This obviously is an abnormal and undesirable operation. Such problems with flame holding consistently occur for hydrogen volume fractions that are over 50%. Higher flame speeds affect flame hydrodynamics defined by the level-set equation. Flame front movement and flashback alters the location of heat release. Movement of the heat release location can change the instantaneous phase between heat release and pressure fluctuations. This can change the thermo-acoustic instability behavior.

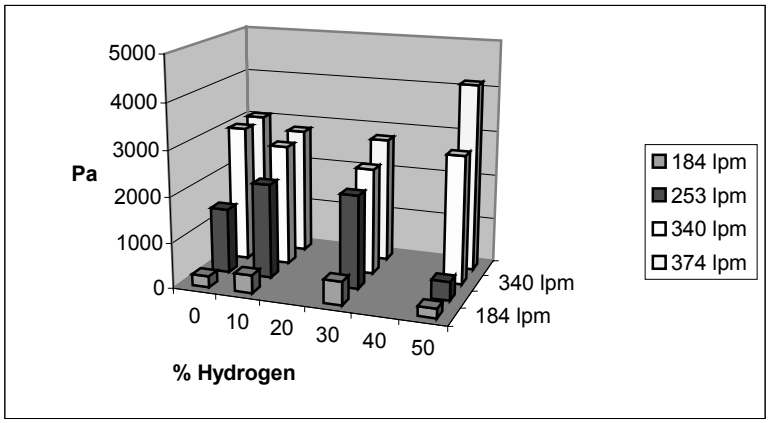

Figure 8 RMS Pressure Amplitude (ϕ=0.7)

Flashback Measurements

Another important phenomenon in the study of pre-mixed flames is flashback. Flow regimes leading to flashback were identified in Figure 3. Flashback can be triggered by acoustic velocity fluctuations and is much facilitated by higher flame speeds. Different fuels therefore have varying degrees of susceptibility to flashback.

A sequence of CH images is recorded showing the flashback cycle using an intensified CCD camera.

For flashback measurements two sensors separated by a distance of $\Delta x = 6.25$ mm are utilized (see Figure 9). Photodiode sensors themselves could not be directly mounted on the walls of the delivery section due to space and heating considerations. However light is transmitted to these photodiodes using fiber optic cables. This specific arrangement not only detects the occurrence of flashback but also enables measurement of its propagation speed.

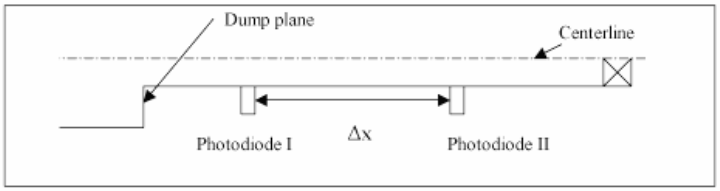

Figure 9 Arrangement for Flashback Speed Detection

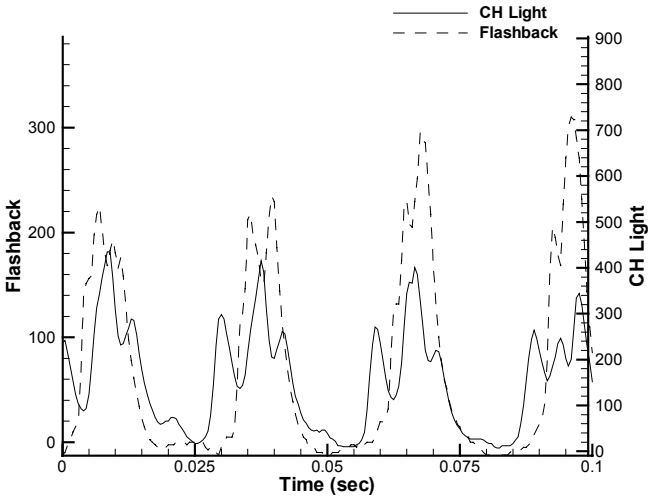

Figure 10 Time History of Heat Release and Flashback Signals (Q_{air}= 340 lpm, ϕ=0.7, 40 % H_2 by vol.)

Figure 10 demonstrates the time histories of heat release and flashback signals. Flashback signal is obtained from the fiber optic cable connected to Photodiode I (see Figure 9). This cable is located about 15 mm upstream of the dump plane level where the flame tip stabilizes normally. Therefore a spike in the heat release signal means that the flame has reached that point during flashback. In the figure one can see the cyclic behavior of heat release due to combustor acoustics. Occasionally spikes are observed in the flashback signal. Note that the flashback signal always lags the CH light signal in time. Flashback signal makes a peak shortly after the CH light signal. There is a very strong temporal coherence between heat release and flashback signals. Strongest coherence is observed at the dominant acoustic frequency.

Figure 11 shows the RMS amplitude of the flashback signal recorded by Photodiode I. Note that for pure methane RMS amplitude has a monotonically increasing trend, which can rather be attributed to the increasing amplitude of limit cycle pressure oscillations. As anticipated there is a lot more flashback activity going on when methane is blended with hydrogen, which is indicated by the peaks in the corresponding region in the graph.

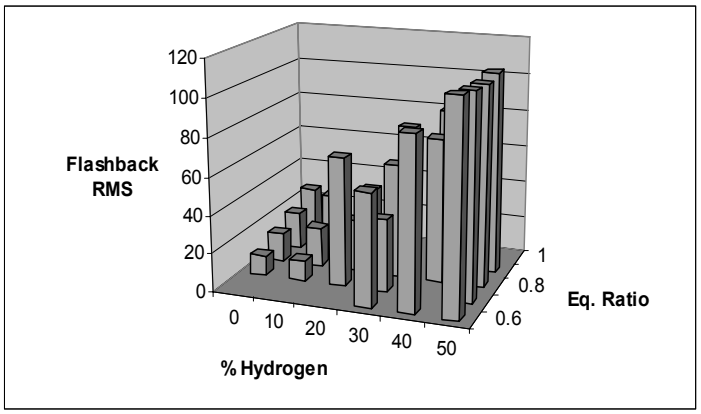

Figure 11 RMS Amplitude of the Flashback Signal (Q_{air}= 374 lpm)

Chemiluminescence Measurements

In order to spatially resolve the temporal heat release characteristics in the main reaction zone, chemiluminescence measurements of the CH radical were performed. The CH radicals have been shown to be representative of the flame front and CH intensity correlates well with the local heat release [21]. An intensified CCD camera with a 512x512 pixel resolution was utilized to acquire the images. The spatial resolution of the corresponding images (see Figure 12) is roughly 135 μm/pixel. The gate duration for the image acquisition was set to 0.10 μs.

A filter mounted on the camera lens is used to transmit the light at λ=430 nm which corresponds to the $B^2\Sigma^-$-$X^2\Pi$(0,0) emission band of the CH radical [22] and to attenuate all other wavelength contributions. A piezoelectric pressure transducer mounted on the combustor wall provided the phase information. Signal from the pressure transducer is fed into a data acquisition board and the trigger signal is generated at the selected phase angle to trigger the image acquisition. To resolve the complete cycle at each phase angle a known time delay is added to the pressure signal. At each triggering condition a sequence of 50 images were recorded. These sequences are then averaged to yield the corresponding mean intensity field.

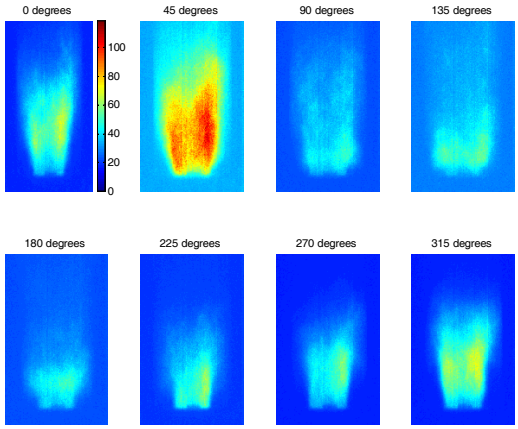

Figure 12 Phase Locked CH Radical Intensity Images (Q_{air}= 340 lpm, ϕ=0.7, 40 % H_2 by vol.)

Figure 12 shows phase locked CH images with 45-degree phase intervals on a false color scale. Conical flame initiation front can easily be distinguished from these CH intensity images, as this radical is a good marker for a methane flame front. In addition, CH radical concentration positively correlates with heat release. This particular floe condition at which these images are recorded demonstrates flashback instability. Flame is conical and attached at 0-degree phase angle with respect to acoustic pressure fluctuations. At the next frame (45-degrees) peak heat release is observed, which is evidenced by the large red zone right downstream of the flame initiation front (the interface between blue and green colors). After peak heat release flame de-attaches from the center body tip and starts propagating upstream. For 180-degree phase instant combustion almost entirely takes place inside the pre-

mixing zone as seen in the corresponding frame on the lower left corner.

Emission Measurements

Nitric oxide emission levels were measured and documented for a number of experimental test conditions. Nitric oxide emissions were measured using a chemiluminescence analyzer. A custom made water-cooled suction probe is inserted into the combustion chamber.

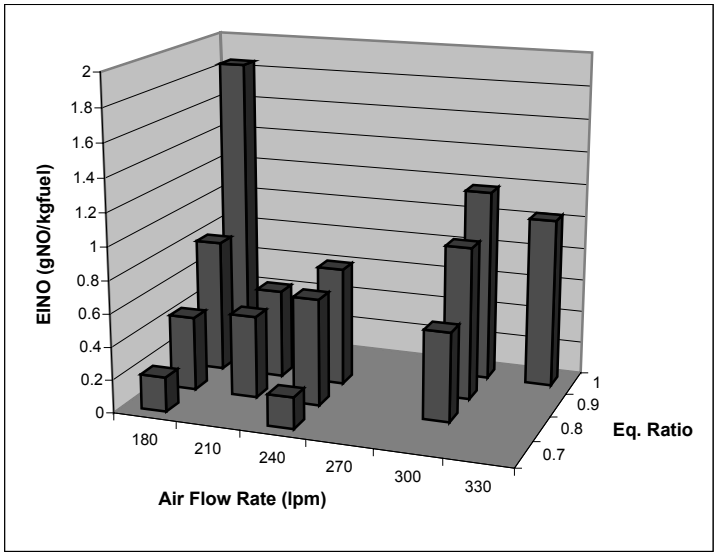

Figure 13 NO Emission Index for Pure Methane

Modern industrial natural gas fueled combustors can produce NO levels below 10 ppm as they operate very close to lean blowout limits in order to drive the adiabatic flame temperature down. Figure 13 shows nitric oxide emissions

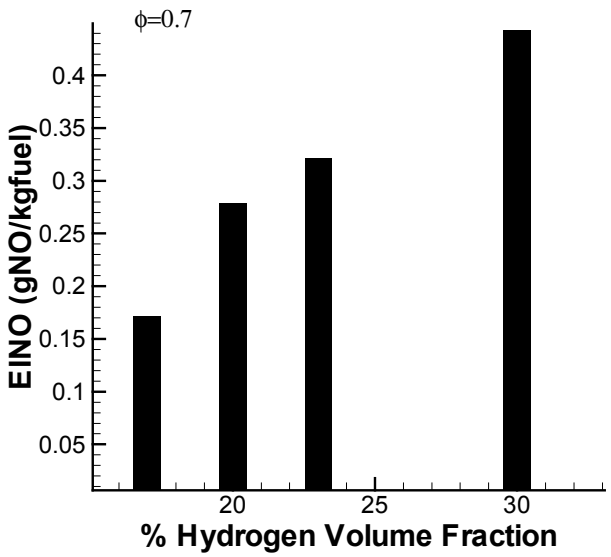

Figure 14 Effect of Hydrogen Enrichment on Emissions Index Q_{air}=292 lpm

index EINO for pure methane in order to establish a baseline for hydrogen enriched studies. Emissions index is defined as grams of nitric oxide generated per kilogram of fuel burnt.

During the experimental study it is observed that keeping the other variables constant and increasing the hydrogen volume fraction of the fuel results in increased nitric oxide emissions index values (see Figure 14). On the other hand hydrogen enrichment enables the sustainment of combustion at much leaner equivalence ratios than that are ever possible with methane (see Figure 15). Premixed lean combustion has long been appreciated as an industry standard technique to reduce nitric oxide emissions. Even though hydrogen addition increases NO_x emissions at a fixed equivalence ratio the overall emissions still can be greatly reduced by burning leaner mixtures of methane and hydrogen blend, which were impossible for the pure methane case. This will reduce the adiabatic flame temperature further down reducing the thermal and other contribution to the total NO_x emissions index.

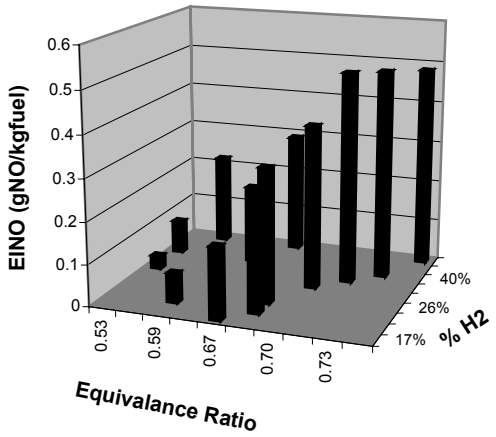

Figure 15 Effect of Hydrogen Fraction and Equivalence Ratio at a Fixed Air Flow Rate Q_{air}=292 lpm

In this section the effect of hydrogen enrichment on nitric oxide emissions are discussed so far. Measurements regarding carbon monoxide emissions have not been conducted but are planned for the near future. However, it is possible to make a few comments on this issue in the light of existing open literature. First of all it is well known that there exists a trade-off between NO_x and CO emissions when traditional hydrocarbon fuels are burnt. Morris et. al. have conducted tests at full pressure and full temperature with hydrogen addition to natural gas. Their results indicate that blends of up to 10% hydrogen by volume showed reduced CO emissions with increased hydrogen addition under lean conditions and moreover they indicate lower NO_x emissions for a given CO emission level. In this study hydrogen methane blends of up to 50 % hydrogen content by volume are investigated yet similar results regarding CO can be expected of this study as well. Furthermore, the aim of hydrogen enrichment is to eliminate CO and UHC emissions in the long run as hydrogen enrichment of natural gas serves as a transition to hydrogen fuel [24].

Flashback Simulations

In this section simulation results of coupled acoustic and hydrodynamic equations are presented in detail. Time integration is stopped in each case only after a stable limit cycle is reached. Due to the non-linearity (saturation effect) in the heat release equation a limit cycle oscillation is quickly established starting from an arbitrary initial condition (see Figure 16). Furthermore, amplitude of this limit cycle depends on the combustor operating conditions. Frequency of this limit cycle is governed by the dominant acoustic mode of the combustor. Peaks observed around 140 Hz. in Figure 17 correspond to this dominant mode for that particular operating condition that they correspond to. As mentioned earlier a single acoustic mode is assumed to be present within the combustor as it can be seen from the Fourier spectra. Mode shape $\psi(x)$ of the pressure wave is given by Eq. 9. The small peak at the third harmonic of the dominant mode (420 Hz.) seen in the heat release spectra is a direct result of the non-linearity in the heat release equation. However, energy contained in this harmonic is much smaller in comparison to the dominant mode. Modes corresponding to higher natural frequencies do not get excited due to the first order filter nature of the heat release equation.

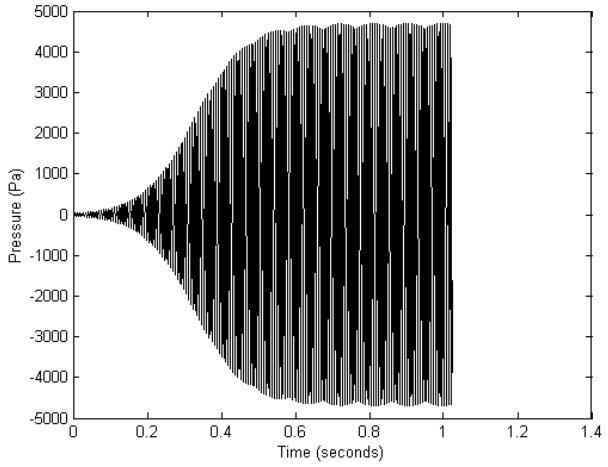

Figure 16 Development of Limit Cycle Pressure Oscillations from an Arbitrary Initial Condition (ϕ=1.0, Q=540 lt/min at x/L=0.85)

Figure 18 demonstrates the phase locked (with respect to pressure) position of the flame initiation front obtained from numerical simulations. Position of the flame front is shown at 90-degree phase intervals. For this case the ratio of laminar flame speed and mean axial flow u/S_L velocity is 0.6. In a typical pre-mixed gas turbine combustor flame speed Mach number is typically one order of magnitude less than the Mach number of the oncoming fluid flow, similar to the case investigated here. Position of the flame front is determined by solving Eq. 14 numerically. Owing to high frequency fluctuations flame front does not experience excessive curvature, consistent with Dowling's observations. Note that Figure 12 showed the phase locked position flame front experimentally. In this regard there is a correspondence between these two figures. It is seen from the figure that almost all the time flame is inside the pre-mixing section moving up and down as in the case of experiments. Only around 270-degree phase instant flame attaches the tip of the center-body (injector) briefly and de-attaches again. During this limit cycle oscillation flame reaches its maximum propagation distance around 90-degree phase instant at which heat release is at its peak point.

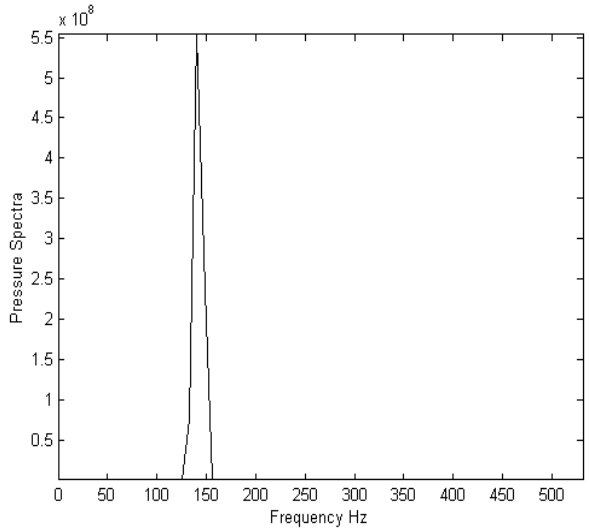

a. Pressure

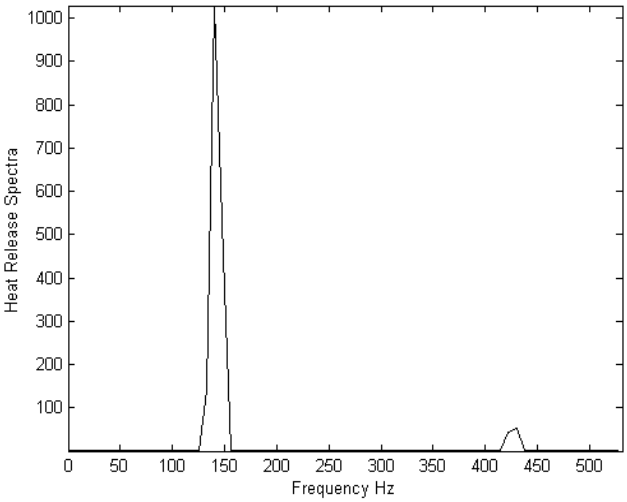

b. Heat Release

Figure 17 Pressure and Heat Release Spectra Corresponding to Figure

Flame propagates up to a non-dimensional distance of z/R=-0.35 which is rather significant, at an instant where peak pressure is reached. This distance on the other hand is rather dependent on the operating condition. On the contrary flame tip is closer to the dump plane when dynamic pressure is at its minimum.

As in the actual combustor the amplitude of limit cycle oscillations from the simulations depend heavily on the operating conditions. As shown both experimentally and numerically, flashback is directly linked with the amplitude of these thermo-acoustic limit cycle oscillations. The more intense the pressure fluctuations are, the more upstream distance the flame tip travels during the flashback instability cycle. A change in operating conditions does not affect the combustor acoustics represented by the transfer function $\eta(s)/q(s)$ significantly. On the other hand the filter

coefficients α, β appearing in Eq. 19 are quite sensitive to the changes in the operating condition. Particularly the gain β of this transfer function has a determining effect on the amplitude of these oscillations. This is because β controls the amount of unsteady heat release input into the acoustic oscillator equation (Eq. 7) is receiving.

Following figure (see Figure 19) shows the RMS amplitude of limit pressure fluctuations obtained from the simulations. RMS pressure amplitude is plotted versus the inlet volumetric flow rate and equivalence ratio. Figures are shown for pressure recorded at x/H=0.85. Recall that locations upstream will experience more intense fluctuations due to the pressure mode shape of the pressure wave. The qualitative trends observed Figure match with the trends observed in the actual laboratory combustor. First of all, as the volumetric flow rate is increased root mean square pressure amplitude increases substantially. This observation is consistent with the experiments. As there is more fuel is burned at higher flow rates there is unsteadier heat release and this yields in higher RMS fluctuations. In mathematical terms at these flow conditions the term the right hand side of Eq. 19 is larger which gives rise to higher heat release. RMS pressure amplitude is less sensitive to changes in the equivalence ratio in comparison to flow rate. Nevertheless, there is a slight increase in pressure fluctuation amplitude with increasing equivalence ratio. This increase can be attributed to the increase in the filter gain β appearing in Eq. 19. Note that this parameter is closely related with the forward reaction rate and the forward reaction rate increases as the equivalence ratio increases until it reaches stoichiometric condition where the reaction proceeds fastest.

The more intense the pressure fluctuations are the more upstream flame propagates during the instability cycle. Of course flashback is facilitated by higher flame speeds, however it is observed that acoustic velocities are typically an order of magnitude larger than laminar flame speeds. Therefore, flashback is mostly related with pressure perturbations. Flame speed, which is proportional with the reaction rate, manifests itself in the filter gain β appearing in Eq. 19. This is the reason why, at larger flame speeds (larger β thus more intense fluctuations) flashback activity is more intense.

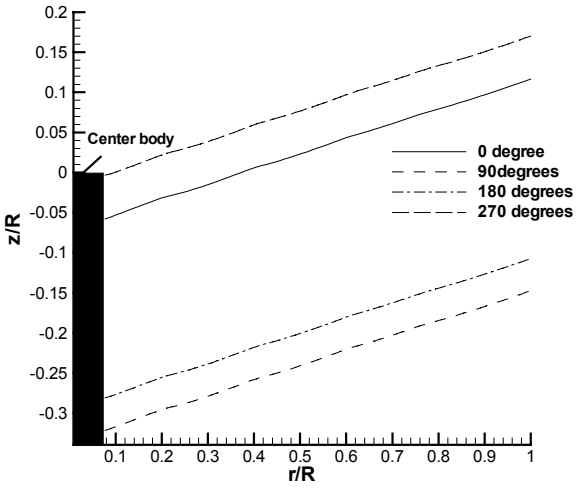

Figure 18 Phase Plot of Flame Tip Location with Respect to Pressure Oscillations Corresponding to Figure

CONCLUSION

A mathematical model has been developed in order to identify the thermo-acoustic instability induced flame flashback and flame holding characteristics. In addition, experiments were conducted using syngas of varying composition and methane gas as the fuel gas. Generally good agreement is observed between theory and experiments. Following is an itemized list of most important conclusions that can be inferred from this study.

1. Thermo-acoustic instability induced flashback could be realistically simulated using the developed mathematical model. A stable limit cycle whose amplitude is dependent on flow conditions is observed due to the non-linearity between velocity and mass flow perturbations.

2. Hydrogen addition to methane extends lean flammability limits enabling combustion at a lower adiabatic flame temperature, which helps reduce NO emissions. Aside from that fact, keeping other variables of interest fixed H_2 enrichment increases emission levels.

3. Hydrogen enrichment can also cause a sudden shift in the combustion regime (i.e. dominant frequency and mode shape). Mechanism leading to this shift should be explored in detail.

4. Significant flame holding problems were encountered with hydrogen rich (i.e. hydrogen volume fraction greater than 50%) fuel mixtures. Therefore pure H_2 could not be oxidized with this combustor arrangement. For such mixtures it is observed that the flame front is not a conical surface attached at the tip of the center body. Rather the flame appears to stabilize inside the pre-mixer near the fuel discharge holes of the injector.

5. In order to prevent the occurrence of flashback attention should be focused primarily on killing the low frequency pressure fluctuations. Note that low frequencies are usually associated with the Helmholtz mode. Because period of oscillation associated with these frequencies are larger and enables the flame front to move further upstream during the flashback cycle.

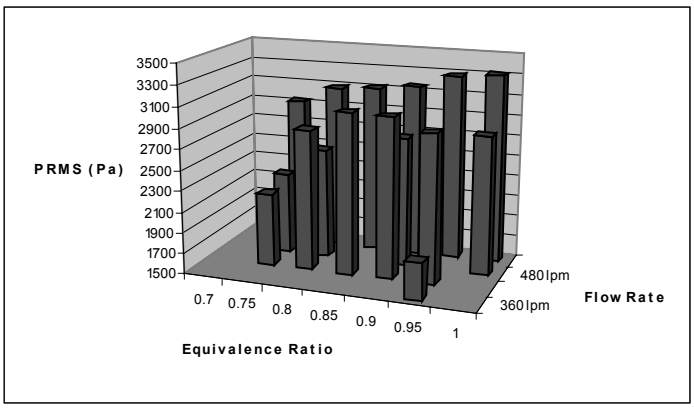

Figure 19 RMS Amplitude of Limit Cycle Pressure Oscillations Recorded at x/L=0.85

Future work aims to develop active control schemes so as to stabilize the flame movement. It is concluded that flashback is primarily triggered by thermo-acoustic instability. An active control scheme designed to suppress the amplitude of thermo-

acoustic limit cycle oscillations is also anticipated to help resolve the flashback issue. Another research prospect is to couple this model with a multi-step reduced chemical kinetics scheme for hydrogen carbon monoxide and methane mixtures and study the effect of acoustics, flame hydrodynamics and mixture composition on nitric oxide and carbon monoxide emissions. A more detailed reaction mechanism would enable a better understanding of these aforementioned phenomena within a single more complete mathematical framework.

ACKNOWLEDGMENTS

This work would not be possible without the financial support obtained from Louisiana Board of Regents Clean Power and Energy Research Consortium. Authors would like to express their gratitude for this support. The help and support received from Mr. Jeffrey Wilbanks in the various facets of the experimental work is gratefully acknowledged.

REFERENCES

1. Lawn, C. J., 1999, "Interaction of the Acoustic Properties of a Combustion Chamber with Those of Premixture Supply", Journal of Sound and Vibration, **224**, pp. 785-808

2. Zimont, V. L., 1979, "The Theory of Turbulent Combustion at High Reynolds Numbers", Combustion Explosions and Shock Waves, **15**, pp. 305-311

3. Dowling, A. P., 1995, "The Calculation of Thermoacoustic Oscillations", Journal of Sound and Vibration, **180**, pp. 557-581

4. Kiesewetter, F., Hirsch, C., Fritz, M., Kroner, M., Sattelmayer, T., 2003, "Two-Dimensional Flashback Simulation in Strongly Swirling Flows", ASME Paper No: GT2003-38395

5. Lord Rayleigh, 1896, "The Theory of Sound", London, Macmillian

6. Tuncer, O., Acharya, S., Banaszuk, A., Cohen, J., 2003, "Side Air Jet Modulation for Control of Heat Release and Pattern Factor", ASME Paper No: GT2003-38853

7. Umurhan, O. M., 1999, "Exploration of Fundamental Matters of Acoustic Instabilities in Combustion Chambers", Center for Turbulence Research Annual Briefs, pp.85-98

8. Lee, D. H., Lieuwen, T., 2003, "Premixed Flame Kinematics in a Longitudinal Acoustic Field", Journal of Propulsion and Power, **19**, pp. 837-846

9. Smoot, L. D., Smith, P.J., 1985, "Coal Combustion and Gasification", Plenum Press, New York

10. Tomzcak, H., Benelli, G., Carrai, L., Cecchini, D., 2002, "Investigation of a Gas turbine Combustion System Fired with Mixtures of Natural Gas and Hydrogen", IFRF Combustion Journal, Article Number: 200207

11. Cowell, L. Etheridge, C., Smith, K., 2002, "Ten Years of Industrial Gas Turbine Operating Experiences", ASME Paper No: GT-2002-30280

12. Mariotti, M., Tanzini, G., Faleni, M., Castellano, L., 2002, "Sperimentazione di Fiamme di Idrogeno a Pressione Atmosferica in un Combustore per Turbogas con Iniezione di Inerti", Technical report, Enel Produzione, Pisa, Italy, ENELP/RIC/RT/-2002/0063

13. Calvetti, S., Carrai, L., Cecchini, D., 2001, "Esecuzione di Prove di Co-Combustione di Gas Naturale e Syngas da Biomassa su un Combustore DLN per Turbina-Gas", Technical report, Enel Produzione, Pisa, Italy, ENELP/RIC/RT/-2001/258/0-IT+RT.RIC.PI

14. Calvetti, S., Carrai, L., Cecchini, D., 2001, "Progettazione di un Combustore DLN Prototipo per TG per la Co-Combustione di Gas Naturale e Syngas da Biomassa", Technical report, Enel Produzione, Pisa, Italy, ENELP/RIC/RT/-2001/146/0-IT+RT.RIC.PI

15. Markstein, G. H., 1964, "Non-Steady Combustion Propagation", The Macmillan Company, Pergamon Press, Oxford, United Kingdom

16. Dowling, A. P., 1999, "A Kinematic Model of a Ducted Flame", Journal of Fluid Mechanics, **394**, pp. 51-72

17. Jones, B., 1974, "Reheat Buzz Film", Combustion Department, Rolls-Royce Derby, United Kingdom

18. Park, S., Annaswamy, A., Ghoneim, A., 2002, "Heat Release Dynamics Modeling of Kinetically Controlled Burning", Combustion and Flame, **128**, pp. 217-231

19. Beer, J.M., Chigier, N. A., 1972, "Combustion Aerodynamics", Applied Science Publishers, London, United Kingdom

20. Yu. G., Law, C. K., Wu, C. K., 1986, "Laminar Flame Speeds of Hydrocarbon Plus Air Mixtures with Hydrogen Addition", Combustion and Flame, **63**, pp. 339-347

21. Bertran, C., Marques, C. S. T., Benvenutti, L. H., 1998, "Mapping of Luminescent Species in a Flame Front", Combustion Science and Technology, **139**, pp. 1-13

22. Garland, N. L., Crosley, D. R., 1985, "Energy Transfer Processes in CH $A^2\Delta$ and $B^2\Sigma^-$ in an Atmospheric Pressure Flame", Applied Optics, **24**, pp. 4229-4237

23. Lieuwen, T., Preetham, 2004, "Nonlinear Flame-Flow Transfer Function Calculations: Flow Disturbance Celerity Effects", 40th AIAA/ASME/SAE/ASEE Joint Propulsion Conference and Exhibit, AIAA 2004-4035, pp. 1-17

24. Schefer, R. W., 2002, "Reduced Turbine Emissions Using Hydrogen Enriched Fuels", Proceedings of the 2002 U.S. DOE Hydrogen Program Review, NREL/CP-610-32405, pp. 1-16

25. Guo, H., Smalwood,G. J., Liu, F., Ju, Y., Gulder, O. L., 2005, "The Effect of Hydrogen Addition on Flammability Limit and NO_x Emission in Ultra-Lean Counterflow CH_4/Air Premixed Flames", Proceedings of the Combustion Institute, **30**, pp. 303-311

26. Zhang, Q., Noble, D. R., Meyers, A., Xu, K., Lieuwen, T., 2005, "Characterization of Fuel Composition Effects in H_2/CO/CH_4 Mixtures Upon Lean Blowout", ASME Paper No: GT2005-68907

27. Morris, J. D., Symonds, R. A., Ballard, F. L., Banti, A., 1998, "Combustion Aspects of Application of Hydrogen and Natural Gas Fuel Mixtures to MS9001E DLN-1 Gas Turbines at Elsa Plant, Terneuzen, The Netherlands", ASME Paper No: GT98-359

